# Development of new family of wide-angle anamorphic lens with controlled distortion profile

Jonny Gauvin, Michel Doucet, Min Wang, Simon Thibault, Benjamin Blanc

Jonny Gauvin, Michel Doucet, Min Wang, Simon Thibault, Benjamin Blanc, "Development of new family of wide-angle anamorphic lens with controlled distortion profile," Proc. SPIE 5874, Current Developments in Lens Design and Optical Engineering VI, 587404 (25 August 2005); doi: 10.1117/12.617505

SPIE.

Event: Optics and Photonics 2005, 2005, San Diego, California, United States

# Development of New Family of Wide-Angle Anamorphic Lens with Controlled Distortion Profile

Jonny Gauvin[a], Michel Doucet[a], Min Wang[a], Simon Thibault[b], Benjamin Blanc[b]
[a]INO, 2740 Einstein Street, Sainte-Foy (Qc), G1P 4S4, Canada
[b]Immervision, 2020 University, Suite 2420, Montreal (Qc), H3A 2H5, Canada

## ABSTRACT

It is well known that a fish-eye lens produces a circular image of the scene with a particular distortion profile. When using a fish-eye lens with a standard sensor (e.g. 1/3", 1/4",.), only a part of the rectangular detector area is used, leaving many pixels unused. We proposed a new approach to get enhanced resolution for panoramic imaging. In this paper, various arrangements of innovative 180-degree anamorphic wide-angle lens design are considered. Their performances as well as lens manufacturability are also discussed. The concept of the design is to use anamorphic optics to produce elliptical image that maximize pixel resolution in both axis. Furthermore, a non-linear distortion profile is also introduced to enhance spatial resolution for specific field angle. Typical applications such as panoramic photography, video conferencing, and homeland/transportation security are also presented.

**Keywords**: optical design, wide-angle lens, anamorphic, distortion control, fish-eye.

## 1. INTRODUCTION

Panoramic imagery and immersive video monitoring find a large variety of applications in architecture, security, and video conferencing. Many of these applications require 180 degrees field of view (FOV) to observe half of the world. The most common lens type that met such a FOV is the fish-eye lens. Fish-eye has the ability to map a hemispheric scene on a sensor by producing a circular image as we can see on Figure 1a. Since commercial sensor format has a 4:3 aspect ratio, one can clearly note that the image does not fill all the sensor area that results in a lost of sensor capacity.

In this paper we present a solution that solves the main drawback of fish-eye. We have designed a new type of Wide Angle Anamorphic Lens (WAAL) that improves pixel coverage of typical 4:3 digital sensor. With an anamorphic design we can produce an elliptical projection of the panoramic scene that fills most of the area of the rectangular sensor. This new design has the particularity to optimize the pixel coverage on the sensor as we can see on Figure 1b. The spatial resolution of standard 4:3 sensor is then increased by about 30% for the large axis. This improvement can be quite useful for some applications requiring high resolution.

This paper also presents another original characteristic introduced in the new wide-angle lens concept. The new lens has the particularity to produce a specific distortion profile. The idea behind this concept is to enhance spatial resolution at specific FOV in order to improve optical performance of the digital imaging system for specific application. As we will see in Section 5, this feature can be also quite benefic for many applications.

## 2. DESIGN APPROACH

Table 1 lists the main requirements of the anamorphic wide-angle lens. One of the basic input data is the sensor characteristic. The selected sensor is a 1/3" CMOS sensor with 1.3 megapixel of resolution; larger format is currently under development. This sensor has an effective area of 4.8 x 3.6 mm with 3.6-µm pixel pitch. Although this sensor is not yet the most common version available in standard video camera, both the technology progress and market evolution will obviously bring this megapixel sensor quite common in a near future. The designed lens must also have a reasonable focal ratio to provide good illumination in reduced light level condition. Although the selected f-number is

Current Developments in Lens Design and Optical Engineering VI,
edited by Pantazis Zakos Mouroulis, Warren J. Smith, R. Barry Johnson,
Proceedings of SPIE Vol. 5874 (SPIE, Bellingham, WA, 2005) · 0277-786X/05/$15

(a) (b)

Figure 1(a): Fish-eye lens generates circular image; (b) Anamorphic lens produces elliptical image.

not quite fast, it is a common standard for commercial fish-eye lens, and will be manageable during optimization process without introducing significant design constraint.

Wide-angle lens produces large field of view by making the image height from the optical axis proportional to the object angle in a similar way to f-theta scan lens. In regular fish-eye lens, this paraxial relation is expressed by

$$y = f \cdot \Theta \,, \qquad (1)$$

where $f$ is the effective focal length of the system, $\Theta$ is the field angle in radian with respect to the optical axis, and $y$ is the image field height. Taking the rectangular shape of the sensor into account, the lens must have different focal length in the two orthogonal axes to maximize the sensor coverage. The anamorphic ratio of the effective focal lengths will then have the same aspect ratio as the sensor itself. From Eq. (1), the effective focal lengths of the anamorphic wide-angle lens are 1.53 mm and 1.15 mm. Some cylindrical lenses will be added in the design to create this anamorphosis.

Table 1: Wide-angle anamorphic lens requirements.

| Requirements | Value |
|---|---|
| Total Track Length | < 60 mm |
| Diameter | < 40 mm |
| FOV | 180º |
| CCD Model | 1/3" CCD |
| Sensor Effective Dimension | X = 4.8 mm, Y = 3.6 mm |
| Resolution | 1300 x 1000 (1.3 MP) |
| Sensor Pixel Size | X = 3.6 μm, Y = 3.6 μm |
| Focal length | EFLx = 1.53 mm, EFLy = 1.15 mm |
| Wavelength | 400 – 700 nm |
| Aperture | F/2.8 |
| Focus | 25 mm to Infinity |

The other feature added to the design is the non-linear distortion profile. Distortion results in a change in the transverse magnification as a function of the image height on the sensor. Traditional fish-eye presents a monotonic variation of the distortion profile as shown in Figure 2a. This curve represents the deviation of the chief ray from the reference paraxial beam as a function of the normalized image height ($y$). Negative distortion means that the real magnification is inferior to the paraxial magnification (Barrel distortion), and vice versa for the positive distortion (Pincushion). Fish-eye lens

will produce barrel-distortion profile and the spatial resolution is then degrading from the optical axis (0 degree) to the extreme FOV (90 degrees).

The new wide-angle lens introduces non-linear distortion to enhanced spatial resolution. Figure 2b shows a typical non-linear distortion we want to produce. In that case the distortion varies in a non-linear way passing from negative to positive values in function of FOV. We will see in Section 5 other possible distortion profiles based on different applications. Table 2 presents the targeted distortion values for some selected FOVs. We also give the pixel coverage (slope). The higher is this number, the better is the spatial resolution. A normalized FOV of 1 corresponds to a viewing angle of 90 degrees. With this profile, the spatial resolution for a FOV of about 0.7 (or 63 degrees) is doubled in comparison to a linear f-theta profile. Figure 3 shows a graphical representation of the distortion profile. Each circle corresponds to the chief ray positions on the detector plane. The circles on the left part are equally spaced. The right part shows some field compression from 0 to 36 degrees and field expansion between 54 and 72 degrees. The anamorphosis is not represented on this figure. During design, it has been assumed that both orthogonal axes will have the same normalized distortion.

The best way to produce and control such a distortion is to add aspheric shape at the front surface of first lens. Since the object numerical aperture (NA) is quite low the frontal lens introduces a very low optical power. The main purpose of this lens is to control the direction of chief ray according to the required distortion profile.

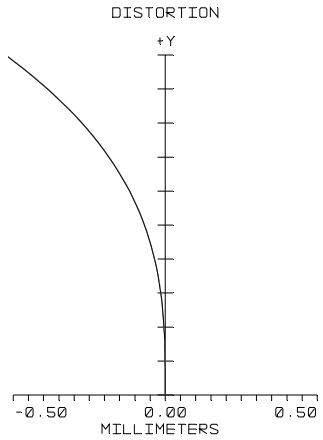


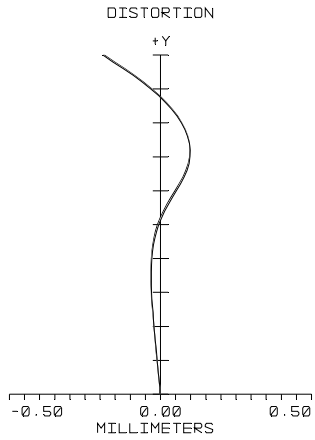


Figure 2: (a) typical fish-eye distortion profile. (b) Non-linear distortion profile.

Table 2 : Targeted distortion values.

| | | | | | | | | | | | |
|---|---|---|---|---|---|---|---|---|---|---|---|
| **Normalized FOV (x)** | 0.00 | 0.1 | 0.2 | 0.3 | 0.4 | 0.5 | 0.6 | 0.7 | 0.8 | 0.9 | 1.0 |
| **Normalized Detector Position (y)** | 0.00 | 0.08 | 0.16 | 0.24 | 0.34 | 0.45 | 0.60 | 0.81 | 0.92 | 0.98 | 1.00 |
| **Slope (dy/dx)** | 0.8 | 0.8 | 0.8 | 0.8 | 1.0 | 1.1 | 1.5 | 2.1 | 1.1 | 0.6 | 0.2 |

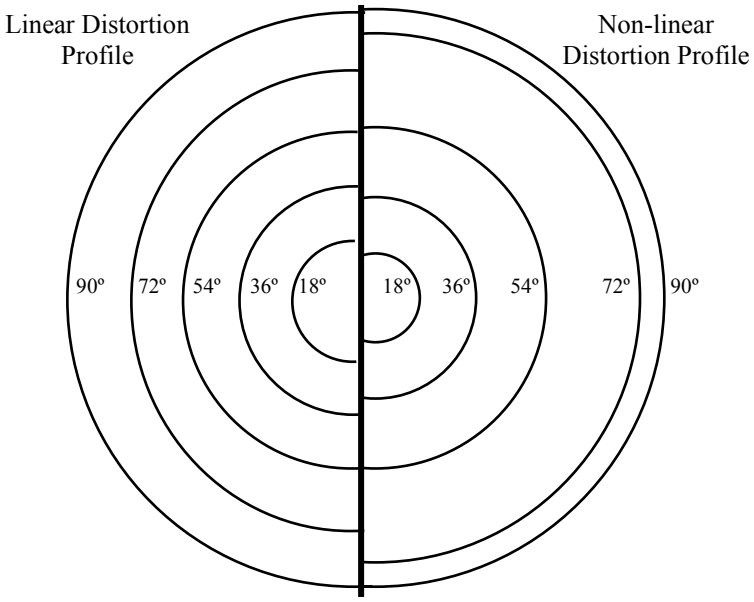


Figure 3: Fields positions on detector area for two different distortion profile.

## 3. DISTORTION OPTIMIZATION

The optimization of the WAAL takes a lot of CPU time especially at the end of the process when the distortion is controlled. The WAAL, like other systems with very large field angles, has significant entrance pupil aberration. The position of the entrance pupil is shifting with the field angle. This forces the use of the robust but slow algorithm for the localization of the entrance pupil and the determination of its size and shape. Moreover, special surfaces are used to control distortion and the aberrations introduced by the anamorphosis. As a result, the ray tracing and the execution of the optimization processes are very slow and is occasionally unstable.

A new method has been developed in order to get a better control of the distortion and to reduce the time of optimization. To increase the speed of the optimization, the process is divided into four steps. Those steps are represented schematically on Figure 4. During the three first steps, the optical system is inverted and the rays are traced starting from the detector. This increases significantly the speed of the ray tracing since the tracking of the entrance pupil position is no longer a problem. The tracking of the entrance pupil for the inverted configuration is easily done by the optical design code because the group of lenses located between the sensor and the pupil do not causes large deviations of the chief rays.

The first step consists in the design of an Anamorphic Very Wide Angle (AVWA) lens. As mentioned before, this is done on an inverted configuration. At this step, the distortion is not controlled and the field of view of the AVWA is only about 65-70% of the desired field of view for the WAAL. Cylindrical lenses are used to produce the anamorphic magnification. As shown on Figure 4a, the image space is supposed to be filled with the same material that composed the first lens of the WAAL. At the exit of the last surface (second surface of the WAAL), the beams should be approximately collimated. This is controlled by means of a perfect (paraxial) lens that focuses the rays to produce spots in its back focal plane. The anamorphosis is controlled in the merit function by forcing the chief ray coming from the object located at the relative coordinate (0,0.75) to arrive on the plane of the perfect lens at the same angle as the chief ray coming from the object point with relative object coordinate (1,0). In the case of the example of Figure 4a, the chief

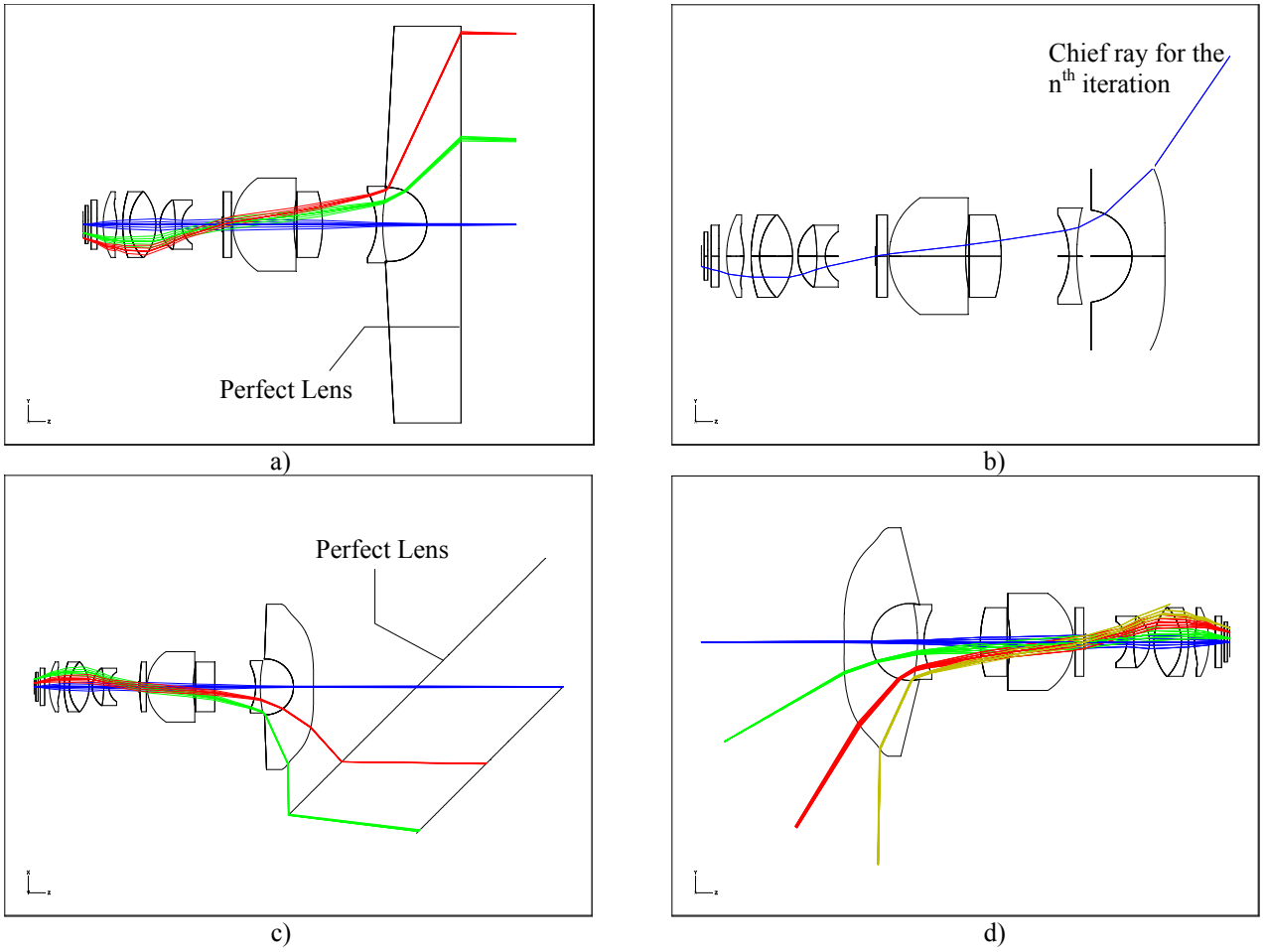


Figure 4: The four steps of the method. The process is done on an inverted configuration for the first three steps. At the first step an Anamorphic Very Wide Angle lens is designed. The thickness of the first lens is infinite and a perfect lens is added. At the second step, an approximation of the first surface is calculated. The result of step 2 is improved at step 3. A tilted perfect lens is used to collect rays that exit the first surface at angle up to 90° from the optical axis. The lens is brought back to its normal orientation of use at step 4 for the final optimization.

ray from the object point located on the vertical axis at 1.8 mm from the optical axis and its counterpart coming from the object point of the horizontal axis at 2.4 mm from the optical axis both arrive on the plane of the perfect lens with an angle of incidence of about 64°.

The second step aims at determining a first approximation for the WAAL first surface. At this stage, the control of the distortion is entirely done with this surface alone. For a wide-angle lens, the beam from a point object is small in comparison to the diameter of the first surface. In fact, the first lens has only small effect on the convergence of the beam and deflects the beam nearly as a prism (see figures 4-1, 4-3 and figures 9-1 to 9-5 of reference 2). Hence, for this step, only the tangential chief rays are considered for the computation. For each field position on the sensor, the angle of the chief ray with respect to the optical axis is known on both side of the first surface. For the sensor side, ray tracing in the inverted configuration designed at the first step determines this angle. On the other side, the angle is given by the imposed pattern of distortion. The angles of the chief rays on both side of the surface and their position of interception with the second surface as a function of the field position are the information required to compute the shape of the first

surface. The computation is done iteratively starting from the center of the surface by a MatLab function. Figure 5 illustrates the computation process for the $n^{th}$ iteration.

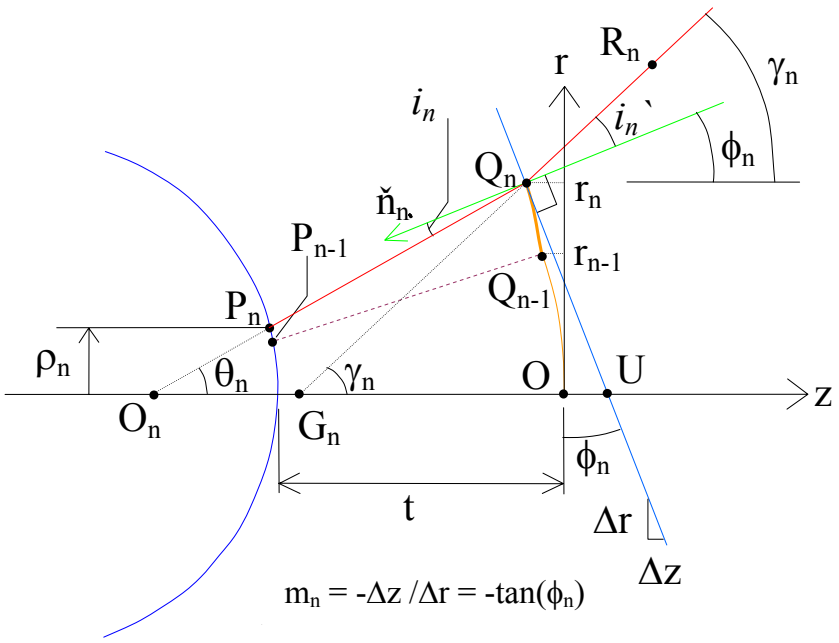


Figure 5: Computation for the $n^{th}$ iteration. The exit angle $\gamma_n$ of the chief ray is known from the imposed distortion curve while its angle $\theta_n$ after the refraction by the second surface is computed by ray tracing. The trajectory of the chief ray includes points $P_n$, $Q_n$, and $R_n$

On Figure 5, the chief ray for $n^{th}$ field position leaves the second surface from point $P_n$. The equation of the line coincident with the path of the $n^{th}$ chief ray inside the first lens is $z = s_n r + w_n$ , where $w_n$ is the z coordinate of the point $O_n$. Let $Q_n$ be the interception point of the $n^{th}$ chief ray with the first surface. At this iteration, the shape of the first surface is known from the origin $O$ up to the point $Q_{n-1}$. The profile of the surface between points $Q_{n-1}$ and $Q_n$ is defined with a second order polynomial $f(r) = a + b\,r + c\,r^2$. The problem to be solved involves four unknown parameters, that is the three parameters of the polynomial and the position of the point $Q_n$. Four equations are thus required to solve the problem:

$$f(r_{n-1}) = a + b\,r_{n-1} + c\,r^2_{n-1} = z_{n-1} \quad (2\text{ a})$$
$$f(r_n) = a + b\,r_n + c\,r^2_n = s_n r_n + w_n \quad (2\text{ b})$$
$$f'(r_{n-1}) = b + 2\,c\,r_{n-1} = m_{n-1} \quad (2\text{ c})$$
$$f'(r_n) = b + 2\,c\,r^2_n = m_n \quad (2\text{ d})$$

For these equations, $f'$ is the derivative with respect to the $r$ coordinate, $z_{n-1}$ is the known z coordinate of the point $Q_{n-1}$ , $r_{n-1}$ and $r_n$ are the radial coordinate of the points $Q_{n-1}$ and $Q_n$ respectively while $m_{n-1}$ and $m_n$ are the slopes of the line that is tangent to the curve at point $Q_{n-1}$ and $Q_n$ respectively. The slope $m_{n-1}$ is known from the previous iteration and $m_n$ is deduced from the Snell law. From Figure 5 and since the line including the points $Q_n$ and $U$ is the tangent to the curve at the point $Q_n$ and $\check{n}_n$ is the normal to the surface at this point, the difference of the angles $\theta_n$ and $i_n$ is equal to the angle $\phi_n$. Moreover, it is evident from the Figure 5 that $\theta_n - i_n = \gamma_n - i'_n$. From this relation, it is easy to prove that

$$tan(i_n) = sin(\gamma_n - \theta_n) / [n - cos(\gamma_n - \theta_n)]. \quad (3)$$

where $n$ is the index of refraction. The last relation gives the angle of incidence $i_n$ and finally the value of $m_n$ is given by

$$m_n = - \tan(\phi_n) = - \tan(\theta_n - i_n). \quad (4)$$

After some algebra, the solution of the problem is given by the set of the following equations

$$c = [(m_{n-1} - m_n)(m_{n-1} + m_n - 2\, s_n)]/[4(z_{n-1} - w_n - s_n\, r_{n-1})] \quad (5\text{ a})$$
$$b = m_{n-1} - 2c\, r_{n-1} \quad (5\text{ b})$$
$$a = z_{n-1} - m_{n-1}\, r_{n-1} + c\, r^2_{n-1} \quad (5\text{ c})$$
$$r_n = r_{n-1} + (m_n - m_{n-1}) / 2c \quad (5\text{ d})$$

Such a piece-by-piece construction guarantees that the profile and its first derivative are both continuous. The final operation of the process is the conversion of the piecewise polynomial into an Even Asphere. This is necessary since the piecewise polynomial used to represent the profile of the first surface is not accepted by the optical design code. The final result is only an approximation of the 'exact' profile. The difference between the fitted Even Asphere and the computed profile generally increases with the value of the radial coordinate.

The curvature of the first surface computed at the second step is generally small for zones of sizes comparable to the size of the beams. This is generally the case, except for certain regions where the distortion correction is highly non linear. For those regions, the first surface affects not only the distortion but it also changes significantly the divergence of the beams. Moreover, those regions are located in the border of the lens where the difference between the piecewise polynomial and its fit as an Even Asphere becomes significant. The third step is a re-optimization of the configuration resulting from the second step. The re-optimization is done simultaneously on many parameters of the configuration including the parameters of the first surface. This is done mainly in order to correct the problem of the divergence caused by large variations of the curvature of the first surface. Moreover, it allows to correct for the deficiencies of the conversion of the piecewise polynomial into an Even Asphere. As for the two previous steps, the third step is done on an inverted configuration. A perfect lens is added to the layout to bring the beams to focus on the back focal plane of this lens. The beams exit the inverted WAAL at angles up to $90^o$ with respect to the optical axis. To make sure that it collects all the rays, the perfect lens is tilted at $45^o$ with respect to optical axis. Two configurations are used at this step, one for object points located in the vertical axis only and the other one for the horizontal axis. Operands are used in the merit function to control not only the size of the spots in the focal plane of the perfect lens but also to control both the distortion and the anamorphosis.

After the first three steps, the configuration must be close to a reasonable solution. At the fourth and last step of the process, the optical configuration of the third step is inverted. The configuration corresponds then to a suitably oriented WAAL. The configuration is optimized again. For this optimization, most of the parameters are declared as variable and the merit function is constructed to allow the control of the distortion and the size of the spots as well as the anamorphosis.

Unfortunately, at the fourth step, the optical design code is generally experiencing many problems when the system is brought back to its normal orientation of use. It is not able to calculate the real position of the entrance pupil for the large field angles. The parameters of the first surface must be modified by the user to allow the optical design code to recover the ability to trace rays for all the object fields. An important part of the work done is lost and the optimization that is required to retrieve a reasonable configuration involves a long computing time. The new method allows some time savings but not as much as expected because of the difficulties encountered by the optical design code to perform ray tracings in the system.

An improved version of the method was also implemented. The difference with the method presented previously is only at the level of the second step. In the improved version, the iterative method is applied not only to compute the shape of the first surface of the first lens but also to compute the shape of its second surface. At the $n^{th}$ iteration, the amount of deviation for the chief ray that has to be produced by the first lens is computed from the known direction of the chief ray and its final direction imposed by the desired distortion. The deviation is divided onto the two surfaces with proportions given by a sharing function that takes values from 0 to 1. The computation is done a first time to determine the piecewise polynomial for the second surface and then a second time for the first surface. For this application, the sharing function is defined by an optimization process. It is defined as a parametric function. At each iteration of the optimization process, the first lens is computed and the merit function is evaluated. The parameters of the sharing

function are adjusted by the optimization process to minimize the value of the merit function. A very simple merit function had been used for this application. It measures the divergence of the beams (one beam for each object position) and computes the difference between the maximum and minimum values for the entire set of the sampled object positions (~1000).

## 4. OPTICAL PERFORMANCES

The long-term goal of this project is to design a complete family of anamorphic wide-angle lens to cover a large variety of application. Until now, we have designed 2 versions of this lens. One is designed using only plastic materiel for high volume production and the other use glass material for lower quantity. Only the glass version has been produced from now.

Figure 6 shows the design of the all-plastic version. It is composed of 8 lenses made of a combination of Zeonex and polycarbonate. Three lenses have aspheric shape, 3 of them are cylinders to provide anamorphosis, and the last 2 are spherical surfaces. Note the typical shape of the front lens that provides the desired distortion. Figure 7 shows the theoretical performances of this lens. We see that the spot diagrams are quite close to the diffraction limit and exhibits little transverse chromatic aberration. The performance is also well demonstrated with the MTF curves. The cut-off of 140 cycles/mm is to the Nyquist frequency corresponding to the current detector pixel size of 3.6 µm. At Nyquist spatial frequency the contrast is still about half of the diffraction limit value and is quite uniform over all FOVs. This lens has not been manufactured yet. However, considering the current manufacturing capabilities of injection molding technology we do not expect any major issue with this design.

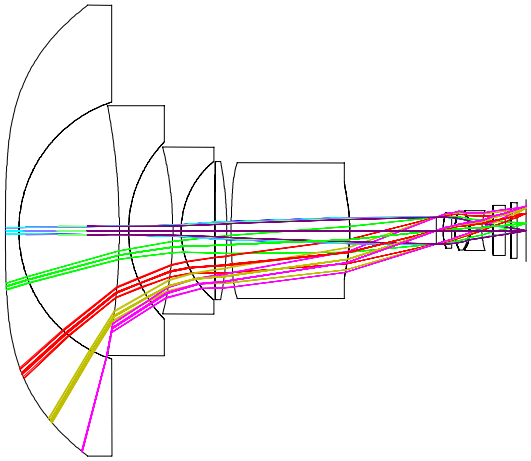

Figure 6: All plastic version of the wide-angle lens.

Figure 8 presents the glass version of the anamorphic lens. This design has been created for low volume production. It consists of 2 aspheric, 2 cylinders, 2 doublets, and 2 standard lenses. Although the original intention was to produce an all-glass version, we have taken the decision to use plastic for the small aspheric lens close to the detector plane. This lens has been manufactured by diamond turning to reduce manufacturing cost of the first prototypes. Figure 9 presents the optical performances of this lens. As we see, the theoretical performances are not as good as the all-plastics version but were good enough for a lab demonstration. The only optical adjustments available in this assembly were the translation of the last 2 lenses within their sub-assembly and for course the focus. Figure 10 presents the first light of the first prototype. The preliminary characterization shows 20% of resolution degradation compared to the theory and the distortion curve is quite close to the expectation.

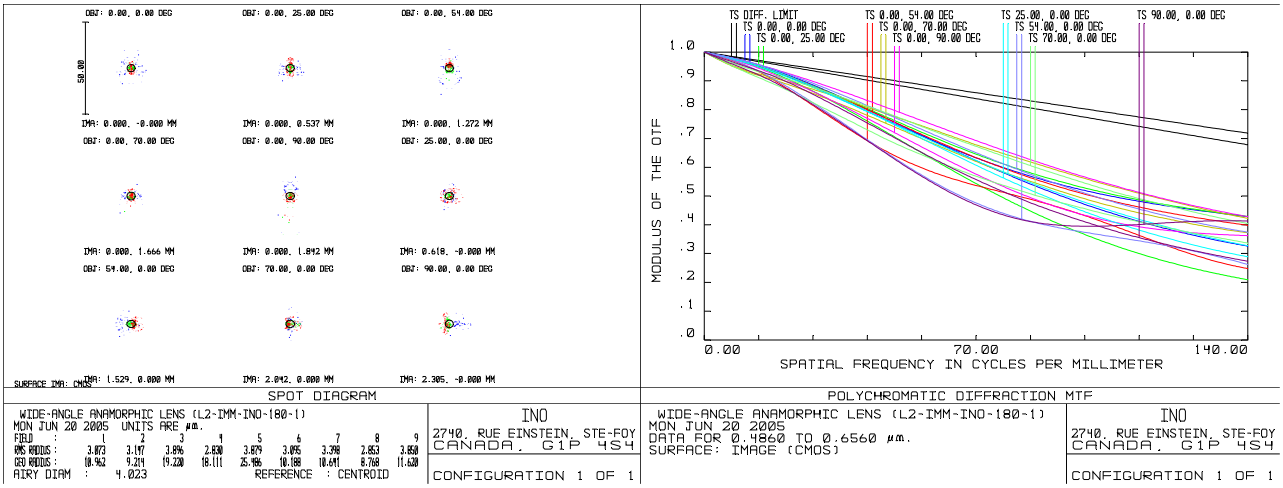


Figure 7: Optical performance of the all-plastics anamorphic lens.

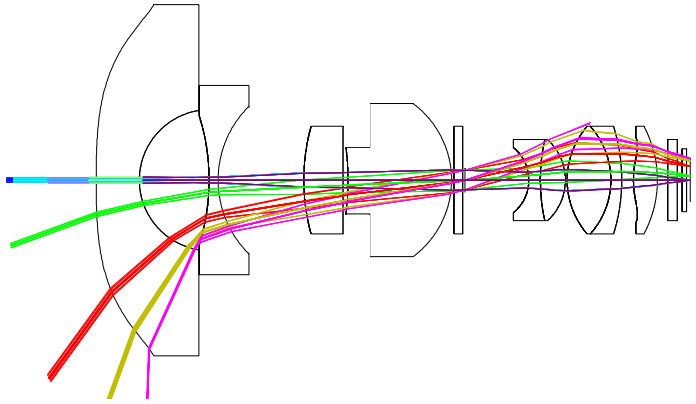

Figure 8: glass version of the anamorphic wide-angle lens.

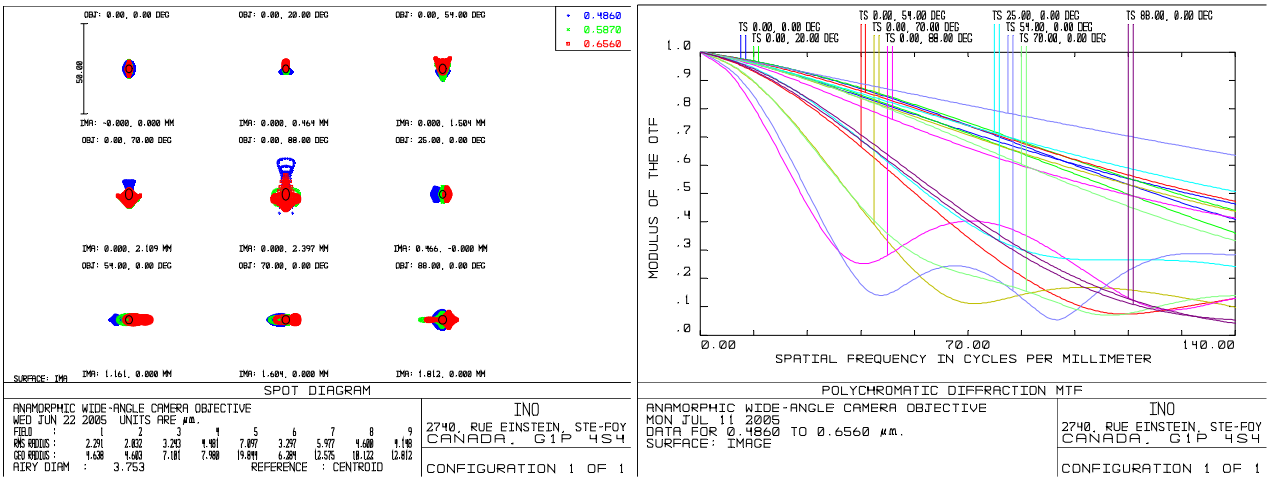


Figure 9: Optical performance of the glass anamorphic lens.

Figure 10: First image with an amorphics wide-angle lens.

## 5. APPLICATIONS

For video surveillance of offices, stores, indoor parking, houses, the camera is usually mounted on the ceiling, its lens facing down as shown in Figure 11 (left picture). The most significant and often distant objects are in the zone at the periphery of the lens (shaded section). This part of the space is the most important because it allows recognizing faces. To maximize the optical performance, the lens is designed to increase the picture resolution in this particular region (see Figure 11 right graph). The dashed line represents the pixel coverage for an ideal fisheye that is constant with the field angle. The solid line is the new pixel coverage obtained by proper distortion control. By controlling the slope of the distortion profile, we can impose a section with higher resolution. If we compare this new kind of optical component performance with the fish-eye lens, an improvement factor up to two in resolution can be achieved.

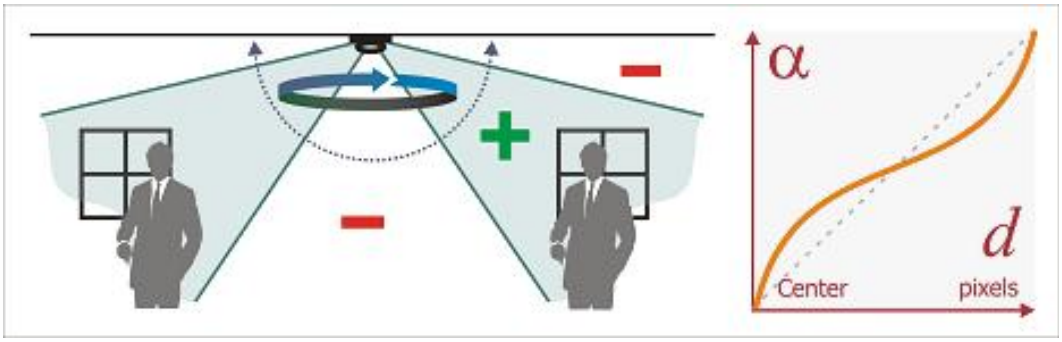


Figure 11: Indoor Video Surveillance (periphery increased resolution)

There are other interesting applications that can benefit from distortion control. To make video-conferencing as efficient as a normal face to face meeting, the same camera can be placed on the table, its lens now facing up as shown on Figure 12. The distortion profile of the lens will help to increase the resolution where the heads of the people are normally positioned.

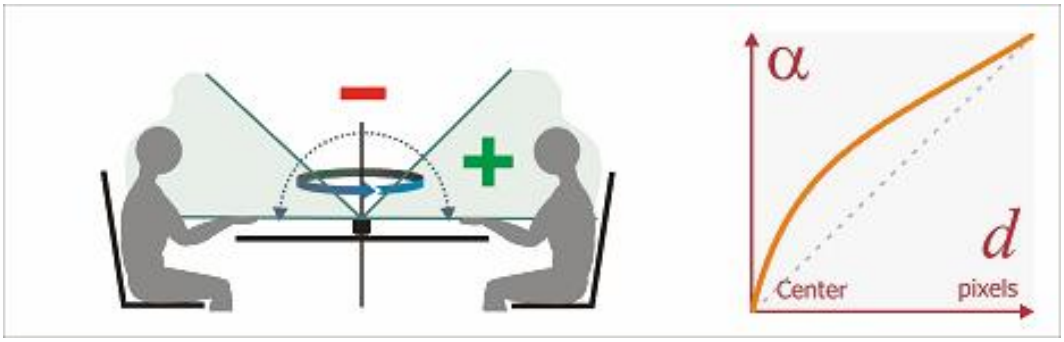


Figure 12: Video-conferencing (periphery increased resolution).

In contrast, some wide-angle lens applications may require that the resolution should be higher in the area in front of the lens such as ATM surveillance applications. For ATM surveillance, it is important to know what happens around the ATM to improve the efficiency of the security but most important information is in front of the camera (to recognize the person). So a wide-angle lens with center-increased resolution is perfectly suitable for the purpose. We can also imagine that such lens could be used in a mobile phone. This will allow an individual to use his mobile phone to participate in a videoconference. The wide-angle feature allows the person to be always in the field of view of the camera even if he does not handle its phone correctly.

Fish-eye lenses are widely used for most outdoor surveillance scenarios like a 360 degrees video surveillance system,. However, if we use a horizon increased resolution distortion profile, the resolution can be up to 3 times superior to a fish-eye lens as shown in Figure 13. The goal is always to increase the resolution in the field of interest. This also helps to reduce the pressure on the software part by providing efficient imaging system.

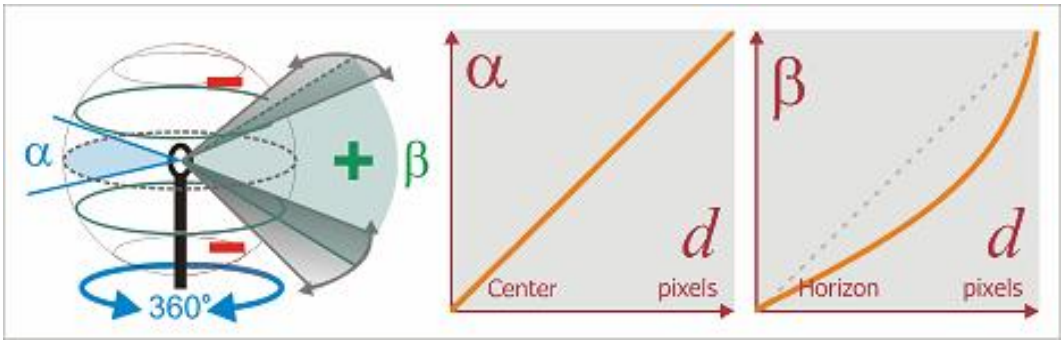


Figure 13: Outdoor 360° surveillance system (horizon increased resolution).

Although the choice of the distortion profile is often complex, there are factors that must always be taken into account: the applications, the minimum acceptable resolution, and the cost. These factors are certainly not independent. Other factors like wavelength range, light level and environment will influence one or more of the three factors. To choose the proper distortion profile for a given application, all information should be considered.

## 6. CONCLUSION

Managing distortion and pixel coverage is an innovative approach in digital imagery. Following this new way of thinking can improve significantly new and existing imagery systems. These new areas of design clearly show that innovation is still useful in optical design. ImmerVision and INO have pushed further the technology by designing and producing a prototype that clearly demonstrates that anamorphic immersive wide angle lens as well as distortion control can be implemented with success. We may have to find a particular wording for this new class of optical objective.

## REFERENCES


1. S. Thibault, Distortion Control Offers Optical System Design a New Degree of Freedom, Photonics Spectra, May 2005.
2. M. Laikin, Lens Design, Second Edition, Marcel Dekker, New York, 1995.